Journal of The Electrochemical Society, **156** (10) D371-D376 (2009)
0013-4651/2009/156(10)/D371/6/$25.00 © The Electrochemical Society

Photoetching Mechanisms of GaN in Alkaline $S_2O_8^{2-}$ Solution

D. H. van Dorp,[a,z] J. L. Weyher,[b,c] M. R. Kooijman,[a] and J. J. Kelly[a,*]

[a]*Condensed Matter and Interfaces, Debye Institute for NanoMaterials Science, Utrecht University, 3584 CC Utrecht, The Netherlands*
[b]*Applied Materials Science, Institute for Molecules and Materials, Radboud University Nijmegen, 6525 ED Nijmegen, The Netherlands*
[c]*High Pressure Research Center, Polish Academy of Sciences, 01-142 Warsaw, Poland*

A study of the electrochemistry of n-type GaN in an alkaline peroxydisulfate ($S_2O_8^{2-}$) solution was used to explain the mechanism of photoetching of the semiconductor under open-circuit conditions. The observed enhancement of the photoetch rate as a result of platinum either directly on or in electrical contact with the semiconductor is shown to be mainly a photogalvanic effect. The factors determining the etching kinetics and surface morphology are elucidated.
 [DOI: 10.1149/1.3183807]

Manuscript submitted January 19, 2009; revised manuscript received June 25, 2009. Published July 27, 2009.

Single-crystalline GaN and ternary group III nitrides attracted huge interest in the scientific community, and their superior chemical and physical properties find application in high performance optoelectronic and electronic devices.[1,2] Etching is an essential step in device fabrication. Dry etching techniques can be used; these include reactive ion etching (RIE), electron cyclotron RIE, inductively coupled plasma RIE, magnetron RIE, and chemically assisted ion beam etching. However, these techniques involve complex and expensive equipment. In addition, dry etching may give rise to damaged surfaces and bulk electronic states, which are detrimental to the performance of optoelectronic devices.[3,4] Wet-chemical etching offers a simple and attractive alternative,[2,5] which avoids the problem of surface damage. The wet etching of GaN and AlN was reviewed by Zhuang and Edgar.[2] The chemical stability of GaN, which results from a large bandgap combined with a low lying valence band (VB) edge, poses a problem for open-circuit etching. Electrochemical etching offers a solution. In a p-type semiconductor, an anodic potential is applied to the semiconductor; holes accumulate at the surface and cause oxidation and dissolution of the solid. Illumination is required for the oxidation of the n-type electrode. However, the necessity of a voltage source for electrochemical etching is, for practical reasons, not always desired.

In 1996, Minsky and co-workers introduced a simple and effective method for photoetching n-type GaN in which the voltage source could be dispensed with.[6] The semiconductor, short-circuited to a Pt "counter electrode" in an alkaline solution, was illuminated with suprabandgap light. This method was subsequently adopted by other groups.[7-10] Depending on the experimental conditions, photoetching could be used to either reveal defects (e.g., threading dislocations leading to characteristic needles) or to etch the surface uniformly. In an electrochemical study, we have shown that the GaN–Pt system operates as a photogalvanic cell and that oxygen in solution plays an essential role.[11] Illumination generates electron–hole pairs in the semiconductor. The VB holes can either recombine with the electrons or cause oxidation and dissolution of the solid. In the latter case, the electrons pass to the counter electrode where they are used to reduce oxygen. To maintain electrical neutrality, the rate of the oxidation reaction at GaN must be equal to the rate of oxygen reduction at Pt. The kinetics of the reaction occurring at the counter electrode is therefore important as this determines the mixed potential of the system. In a potentiostatic experiment in which the potential of the semiconductor is fixed by an external source, e.g., a potentiostat, this is not the case.[5] Photoetching can also be achieved by putting a patterned Pt layer directly on the semiconductor.[12]

A more recent development has involved the addition of a strong oxidizing agent, e.g., peroxydisulfate ($S_2O_8^{2-}$), to the alkaline etchant.[13-16] In 1999, Bardwell et al. showed that the counter electrode could be dispensed with in this solution by the use of a Pt metal pattern on n-type molecular beam epitaxy (MBE) GaN.[13] Etch rates up to 50 nm/min were observed. This system was subsequently studied in more detail, and a mechanism was proposed.[15] Apart from the usual steps required for photoetching of a semiconductor, the authors emphasized the importance of the peroxydisulfate radical anion ($SO_4^{\bullet -}$) resulting from the decomposition of $S_2O_8^{2-}$ either by photolysis or "catalytic decomposition" at Pt. They suggested that the $SO_4^{\bullet -}$ species on reacting with water can produce a hydroxyl radical ($OH^{\bullet}$). These reactive radicals diffuse from Pt to bare GaN where they oxidize the semiconductor. A somewhat similar mechanism involving a photochemical decomposition of $S_2O_8^{2-}$ at Pt in HF solution was proposed by Rittenhouse et al. for the photoetching of SiC.[17] Diaz et al. showed that platinized GaN can also be made porous by etching under UV illumination in a $CH_3OH/H_2O/HF$ solution containing H_2O_2.[18,19] Peroxydisulfate (and hydroxyl) radicals are extremely reactive. It seems unlikely that they would survive transport over the distances required to explain the beneficial effects of the noble metal on photoetching in the studies described above. Our previous study of the photoetching of n-type GaN in an oxygenated aqueous solution led us to suspect that photogalvanic effects might also be important for the peroxydisulfate system. In this paper, we describe a photoelectrochemical study of the etching of GaN in alkaline solutions of $S_2O_8^{2-}$.

The electrochemistry of $S_2O_8^{2-}$ has been investigated at various semiconductor electrodes. This two-electron acceptor belongs to a class of strong oxidizing agents, which at p-type electrodes cause photocurrent doubling.[20] The first step of the reduction requires a conduction band (CB) electron that is generated by a (supra)bandgap photon

$$S_2O_8^{2-} + e^-_{(CB)} \rightarrow SO_4^{2-} + SO_4^{\bullet -} \quad [1]$$

The $SO_4^{\bullet -}$ radical anion is an extremely strong electron acceptor. It extracts an electron from the VB (even of wide bandgap semiconductors); this is equivalent to hole "injection" into the VB

$$SO_4^{\bullet -} \rightarrow SO^{2-} + h^+_{(VB)} \quad [2]$$

Each photon gives rise to two holes (the primary and the injected hole) measured as a photocurrent in the external circuit. At an n-type semiconductor, illumination is not required; Reaction 1 occurs in the dark. In this case, the injected hole (Reaction 2) can recombine radiatively with the majority carriers (CB electrons) to give electroluminescence (EL). Such processes have been observed with GaN and SiC.[21-24] Huygens et al. showed that $S_2O_8^{2-}$ was reduced electrochemically at epitaxial GaN in the dark in a H_2SO_4 solution and that the reaction was kinetically favorable.[23,25] Hung and coworkers observed visible (defect) luminescence from n-type epitaxial GaN in $S_2O_8^{2-}$ at pH 2.7.[24] Similar EL results were reported by Huygens et al. for pH 4. These various results indicate that, as at

* Electrochemical Society Active Member.
z E-mail: d.h.vandorp@uu.nl

other semiconductors, the reduction of $S_2O_8^{2-}$ follows the two-step mechanism (Reactions 1 and 2).

In this paper, we used the results of an electrochemical study of n-type GaN in alkaline solutions of $S_2O_8^{2-}$ as a basis for a consideration of the photoetching of the semiconductor. Three approaches were used: (*i*) photoanodic etching in which the potential of the semiconductor is fixed by a voltage source (potentiostat), (*ii*) photogalvanic etching in which the semiconductor is short-circuited to the counter electrode (no voltage source), and (*iii*) electroless photoetching (without a counter electrode). In a separate paper, we described the results on the optimum $S_2O_8^{2-}$/KOH ratios for revealing defects and for pattern etching or polishing. The reliability of defect-selective etching in $S_2O_8^{2-}$/KOH solutions is also considered.[26]

Experimental

As-grown metallorganic chemical vapor deposition (MOCVD) epitaxial GaN wafers were obtained from Fraunhofer-Institut für Angewandte Festkörperphysik in Freiburg. The layers were 7 μm thick, Si doped, and had a carrier concentration of ~1×10^{18}/cm^3. For the EL measurements, home-grown MOCVD epitaxial GaN layers were used with a carrier concentration of 1×10^{18}/cm^3 and 2–5 μm thicknesses. Ohmic contacts to the GaN were made by evaporating a Ti layer, 100 nm thick, without any additional heat-treatment. All the samples used in this study had a Ga-polar face.

Electrochemical measurements were performed in a three-electrode cell with a platinum counter electrode and a saturated calomel electrode (SCE) as reference. Potentials were given with respect to SCE. A potentiostat (PalmSens, PS-PDA1) controlled by PSLite was used to measure the current–potential curves in the dark and under illumination. The curves were recorded at a constant scan rate of 10 mV/s from negative to positive potential. The short-circuit experiments were conducted in a two-compartment cell. To maintain charge balance, the compartments were connected by a porous glass frit. The current was measured with an HP 3458A multimeter controlled by LabVIEW. The etched depth was determined with a surface profiler (Tencor Alpha-Step). The surface morphology was characterized with a scanning electron microscope (SEM) (Philips XL 30 SFEG operated at 20 keV).

The light source used for the electrochemical experiments was a 450 W xenon lamp with a power supply (Oriel 66924). The UV light was focused on the substrate after it had passed through a water filter.

For the EL experiments, a 0.1 M $K_2S_2O_8$ (purified agent), 0.1 M KOH solution was used. The spectra were recorded with a charge-coupled device camera (Acton Research Corporation, Spectra Pro-300i).

Results and Discussion

Photoelectrochemistry and electroless photoetching of GaN.— Figure 1, curve (a), shows a current density–potential plot of n-type GaN in a 0.02 M KOH solution recorded in the dark. Diode characteristics are observed. Mott–Schottky measurements revealed that the flatband potential (U_{FB}) is located at −1.4 V.[27] At positive potentials (>−1.0 V) corresponding to the majority carrier depletion at the surface, no current is observed. For negative potentials, at which the electron concentration at the surface is high, two cathodic processes occur via the CB: the reduction of oxygen and the reduction of water

$$O_2 + 2H_2O + 4e^- \rightarrow 4OH^- \quad [3]$$

$$2H_2O + 2e^- \rightarrow H_2 + OH^- \quad [4]$$

Reaction 3 occurs in the potential range negative with respect to −1.0 V and is controlled by mass transport of oxygen to the electrode surface. Stirring or aerating the solution increases the current density in this range. Water reduction becomes dominant at potentials lower than −1.6 V (Reaction 4).

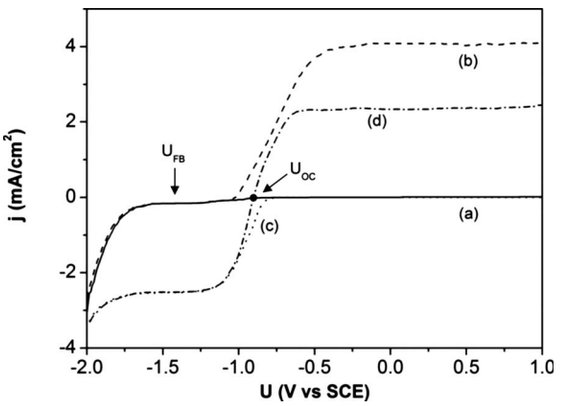

Figure 1. Current density–potential plots for n-type GaN in a 0.02M KOH solution recorded (a) in the dark and (b) under illumination. After addition of 0.02 M $S_2O_8^{2-}$, curve (c) is obtained in the dark, and curve (d) is obtained under illumination. The potential was scanned at a rate of 10 mV/s. The solution was not stirred. U_{FB} is the flatband potential of GaN in KOH solution.

When the electrode is illuminated [Fig. 1, curve (b)], no photocurrent is observed at potentials below −1.0 V. In this range, the electric field of the depletion layer at the surface is not sufficiently strong to separate the electrons and holes; they recombine both in the bulk and at the surface. An increase in photocurrent is observed in the potential range from −1.0 to −0.5 V; here, the partial spatial separation of the charge carriers occurs in the space-charge and diffusion layers. The electrons escape to the external circuit and are measured as current (they cause water reduction at the counter electrode). The holes driven to the surface are localized in surface bonds and cause a dissolution of the semiconductor[11]

$$GaN + 6OH^- + 3h^+ \rightarrow GaO_3^{3-} + 3H_2O + 1/2N_2 \quad [5]$$

At this moderate band bending, the electron concentration at the surface is still rather high, and therefore some recombination occurs mainly via defect states. The crystal surrounding the defects is etched, and the defects are revealed as hillocks.[9] At high positive potentials, >−0.5 V, the band bending is strong and the current density becomes independent of potential. As previously reported for GaAs,[5] Macht et al. found that the photocurrent for GaN in the strong band bending regime (i.e., >−0.5 V) could be controlled either by OH^- ions or by holes (Reaction 3).[11] If the flux of OH^- to the surface is larger than that of photogenerated holes ($\Phi_{OH} > \Phi_p$), then the limiting photocurrent shows a linear dependence on the light intensity. If the hole flux to the surface is larger than that of OH^- ($\Phi_p > \Phi_{OH}$), then the limiting photocurrent depends on the pH of the solution and the hydrodynamics of the system and is independent of light intensity. We found a similar trend in this work. When the mass transport of the OH^- ion determines the kinetics, oxide formation can be expected[28]

$$2GaN + 6OH^- + 6h^+ \rightarrow Ga_2O_3 \quad [6]$$

The gallium oxide dissolves chemically as gallate in the alkaline solution

$$Ga_2O_3 + 6OH^- \rightarrow 2GaO_3^{3-} + 3H_2O \quad [7]$$

The combination of mass-transport control and the presence of a surface oxide gives rise to polishing of the wafer.[5] When OH^- is depleted at the surface, a concentration gradient extends from the surface into the bulk of the solution. Normally, mass transport to protruding parts is enhanced, which results in a leveling of the surface; this occurs when the thickness (δ) of the diffusion layer is of the same order of magnitude as the surface roughness. In an unstirred solution, δ is several hundreds of micrometers and therefore

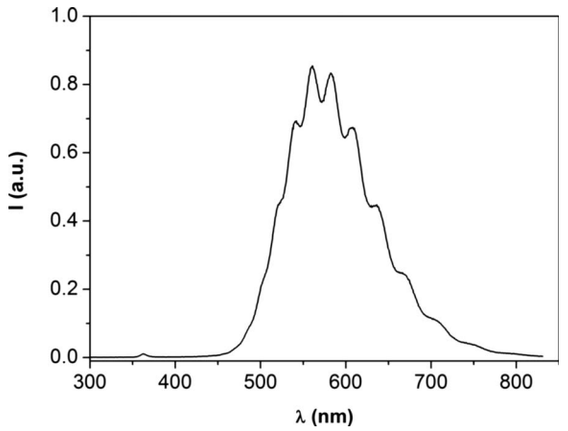

Figure 2. EL spectrum of n-type GaN recorded in a 0.1 M $S_2O_8^{2-}$ solution of pH 13.

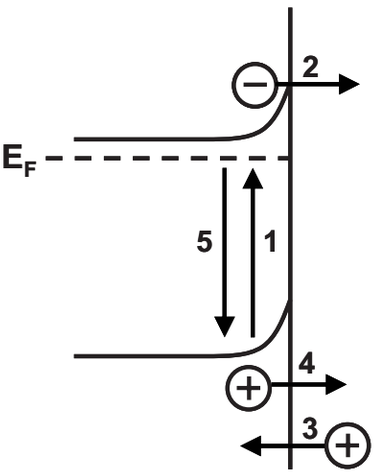

Figure 3. Schematic representation of the steps occurring during electroless photoetching of n-type GaN in a KOH/$S_2O_8^{2-}$ solution. E_F indicates the Fermi level of the semiconductor.

much larger than the surface roughness. Because the rate of photogeneration of the holes is higher than the rate of their reaction at the surface, an accumulation of positive charges occurs at the interface. The potential drop no longer occurs over the space charge layer but instead over the oxide film (ΔU_{ox}).[29] Small variations in oxide thickness give rise to variations in ΔU_{ox}. Locally, where ΔU_{ox} is largest, typically at protrusions, the dissolution rate is enhanced. Such local field-enhanced etching leads to a leveling of the surface. Macht et al. found that at higher pH, the limiting photocurrent at high light intensity became independent of the OH^- concentration. This was not observed in the present work. The reason for this discrepancy is not clear.

Figure 1, curve (c), shows a current density–potential plot of n-type GaN in 0.02 M KOH/0.02 M $S_2O_8^{2-}$ solution recorded in the dark. Again, no current is observed at a positive potential. While the onset of the cathodic reaction occurred at about −1.0 V in KOH solution, we see that after the addition of $S_2O_8^{2-}$, the onset shifts to −0.8 V. At this potential, $S_2O_8^{2-}$ is reduced by CB electrons to form a sulfate ion and a peroxydisulfate radical (Reaction 1). The more positive onset potential shows that the reduction of $S_2O_8^{2-}$ is more favorable than that of O_2 at GaN. From −1.2 to −1.7 V, the current density is independent of potential and is determined by the $S_2O_8^{2-}$ concentration and the hydrodynamics of the system. At potentials below −1.7 V, water reduction becomes important.

The reduction of $S_2O_8^{2-}$ involves hole injection (Reaction 2), as shown by the EL measurements. As previously found at low pH, electron–hole recombination gives rise to light emission in the KOH/$S_2O_8^{2-}$ solution. In Fig. 2, an EL spectrum is shown. Two emission bands are observed: a small peak at 363 nm (3.42 eV) and a large broad peak at 571 nm (2.17 eV). The former is attributed to band–band or exciton emission, and the latter is attributed to defect emission, a shallow donor (O_N), deep acceptor (V_{Ga}) transition.[30] A strong intensity modulation is observed in the defect emission due to interference arising from multiple internal reflection in the GaN epitaxial layer. This suggests that the epitaxial GaN layer acts as a Fabry–Perot cavity. The mode spacing in such a cavity depends on the layer thickness. During etching, the layer thickness could, therefore, be followed in situ by EL measurements. Strong cavity effects are also observed for InGaN/GaN heterostructures on Si substrates.[31]

Figure 1, curve (d), shows that the cathodic current density is not affected by illumination. The current in the anodic range is lower than that observed in curve (b). This was caused by the absorption of high energy photons by $S_2O_8^{2-}$ ions in solution. Absorption becomes significant at wavelengths below 300 nm and peaks at 218 nm. Figure 1, shows that in the $S_2O_8^{2-}$ solution, there is a common potential range in which anodic dissolution and cathodic reduction occur. This indicates that open-circuit photoetching of a nonmetallized GaN film is, in principle, possible. At the open-circuit potential (U_{OC}) of the GaN electrode in the KOH/$S_2O_8^{2-}$ solution under illumination, the rate of photoanodic dissolution is equal to the rate of cathodic reduction. Figure 1, curve (d), shows that U_{OC} is located at −0.9 V (for comparison, the value of U_{OC} in KOH solution is −1.0 V). The etch rate for electroless photoetching is under kinetic control, i.e., governed by the electron and hole dynamics at the interface, as schematically shown in Fig. 3 for an n-type electrode.

On illumination, electron–hole pairs are generated (step 1). The photogenerated electrons can react with $S_2O_8^{2-}$ to give SO_4^{2-} and $SO_4^{\bullet-}$ (step 2). Due to its extreme reactivity and low lying acceptor levels, $SO_4^{\bullet-}$ captures an electron from the VB; i.e., it injects a hole (step 3). The VB holes cause an oxidation and a dissolution of GaN (step 4). The gallate (GaO_3^{3-}) product (Reaction 5) is soluble in an alkaline solution. Apart from reducing $S_2O_8^{2-}$ ions, photogenerated electrons can recombine with VB holes directly or via defect states in the bandgap (step 5). Under steady-state conditions, the Fermi level E_F and the band bending are determined by the electron balance and hole balance at the surface.

Bardwell and co-workers demonstrated an open-circuit photoetching of SiO_2-patterned GaN substrates. They obtained low etch rates (in the order of several nanometers per minute). The surface morphology was, however, poor.[15,32] Hwang et al.[16] showed that by chopping the UV source, an improved surface morphology is obtained. Figure 1, shows that this open-circuit photoetching system is rather critical. A slight shift in either the anodic or the cathodic curve in an unfavorable direction along the potential axis can kill the etch rate. Such a shift can be caused by poor charge-transfer kinetics or enhanced electron–hole recombination in the semiconductor.[11] The latter depends on the dopant and defect density and can vary with the sample.

Photogalvanic etching of GaN.— The original motivation for the work of Bardwell et al.[13] was to eliminate the counter electrode by adding a strong oxidizing agent ($S_2O_8^{2-}$) to the etchant (KOH) to scavenge the photogenerated electrons. Although open-circuit photoetching was observed, the etch rates were low (see above). They found that the etch rate could be increased by depositing a Pt mask on the GaN substrate.[15] This enhancement was attributed to radicals, formed by catalytic decomposition of the $S_2O_8^{2-}$ ions at the noble metal, which subsequently oxidized the semiconductor. The enhanced etch rate could, however, be due to photogalvanic effects. To

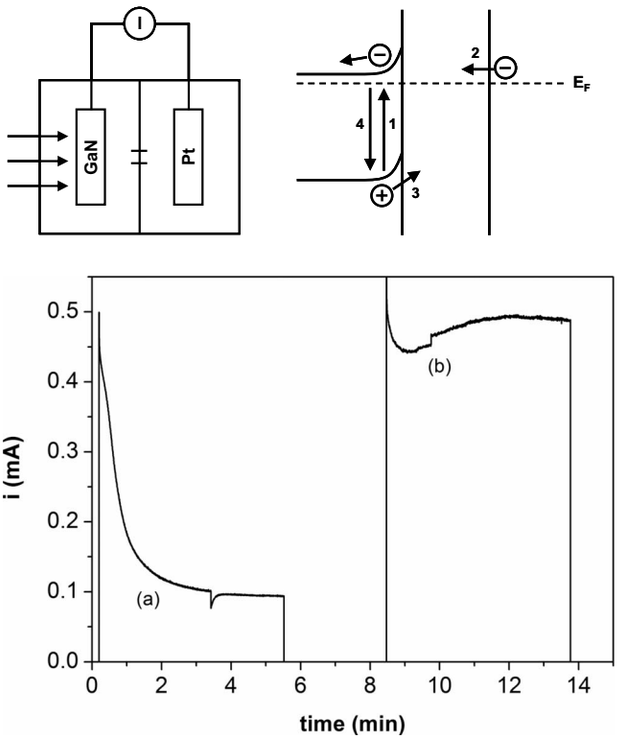

Figure 4. Schematic representation of a two-compartment photogalvanic cell and the corresponding band-energy diagram (top). (a) The photocurrent–time plot was recorded with 0.02 M KOH solution in both compartments. (b) When 0.02 M $S_2O_8^{2-}$ was added to the compartment of the Pt counter electrode, the photocurrent density increased.

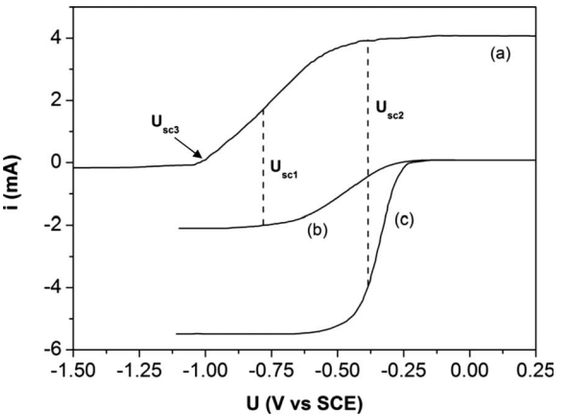

Figure 5. (a) Current–potential plot for photoanodic dissolution of GaN in a 0.02 M KOH solution. (b) Corresponding plot for reduction of $S_2O_8^{2-}$ at a Pt electrode in a 0.02 M KOH/0.02 M $S_2O_8^{2-}$ solution. (c) When the surface area of the Pt is increased, the reduction current increases. The photoanodic curve is corrected for absorption by $S_2O_8^{2-}$.

check this, we used a two-compartment cell in which the n-type GaN electrode was separated from the Pt counter electrode (left side of Fig. 4). No voltage source was used. This cell allowed us to study the influence of $S_2O_8^{2-}$ on the anodic and cathodic reactions independently.

With short-circuited electrodes and no ohmic losses in the system, the Fermi level is constant (see the band-energy diagram in Fig. 4). Upon illumination, electron–hole pairs are generated (process 1, Fig. 4). The electric field of the space charge layer causes electrons to pass via the external circuit to the Pt counter electrode where the reduction of $S_2O_8^{2-}$ takes place (process 2). The electrons are measured as current. The holes are localized in surface bonds and are used for etching (process 3). Holes that recombine with electrons at or near the GaN surface (process 4) do not contribute to etching. In the steady state, the rate of GaN dissolution is equal to the rate of reduction occurring at the counter electrode.

Curve (a) of Fig. 4 shows a current–time plot recorded with 0.02 M KOH solution (unstirred) in both compartments. The area of the GaN electrode was approximately 0.09 cm^2. No current is observed in the dark. Upon illumination, the current increases instantaneously and decays subsequently to a steady-state value of about 0.1 mA. The current is determined by the mass transport of oxygen to the Pt surface and can be enhanced by stirring or increasing the area of the Pt counter electrode.[11] When 0.02 M $S_2O_8^{2-}$ is added to the compartment of the counter electrode, the photocurrent increases by more than a factor of 5 [Fig. 4, curve (b)]. This is not observed when $S_2O_8^{2-}$ is added to the compartment of the GaN electrode (in this case, the current decreases due to light absorption by $S_2O_8^{2-}$). The enhancement of the current is a photogalvanic effect; the etch rate is determined by the rates of the anodic and cathodic processes.

The results shown in Fig. 4 can be understood on the basis of the electrode kinetics of the individual reactions. Figure 5, curve (a), shows the current–potential curve of an illuminated GaN electrode in an unstirred 0.02 M KOH solution [see also Fig. 1, curve (b)]. Figure 5, curve (b), shows the current–potential curve, measured independently, for a Pt electrode in a 0.02 M KOH/0.02 M $S_2O_8^{2-}$ solution. The onset of current due to the $S_2O_8^{2-}$ reduction at Pt is at about −0.25 V. After an exponential increase with decreasing potential, the current becomes constant as a result of mass transport limitation of the oxidizing agent. When the electrodes in the two compartments of the galvanic cell (Fig. 4) are short-circuited, a potential (U_{SC1}) is established, at which the photoanodic current (due to dissolution of the semiconductor) is equal to the cathodic current (due to $S_2O_8^{2-}$ reduction at Pt). This short-circuit potential is in the onset of the photoanodic curve. Curve (c) of Fig. 5 shows the effect of a 2.6-fold increase in the area of the Pt counter electrode. Because of the resulting increase in cathodic current, the short-circuit potential shifts in the positive direction to U_{SC2}, which corresponds to the limiting photocurrent range. In the absence of $S_2O_8^{2-}$, the short-circuit potential of the system is determined by oxygen reduction at the Pt (not shown). This value, U_{SC3}, is considerably more negative than that measured with $S_2O_8^{2-}$ in the counter electrode compartment. This is due to two effects: the low solubility of O_2 in an aqueous solution and the less favorable kinetics for oxygen reduction.

The results shown in Fig. 5 suggest that with the proper choice of experimental conditions, the GaN surface finish can be controlled; the light intensity, OH^- and $S_2O_8^{2-}$ concentrations, the GaN/Pt surface area ratio, and the hydrodynamics determine the short-circuit potential and, thus, the mode of etching. We confirmed this experimentally with some results shown in Fig. 6. The experiments were performed in a single-compartment photogalvanic cell with a GaN:Pt surface area ratio of 1:8. Figure 6a shows an SEM image of a patterned GaN surface, which was etched for 20 min in an unstirred solution of 0.004 M KOH/0.02 M $S_2O_8^{2-}$. A smooth surface is obtained with a surface roughness comparable to that of an as-received sample (see the inset). The etch rate is low (~3 nm/min) and is under mass transport control by OH^- ions ($\Phi_p > \Phi_{OH}$), i.e., "polishing" conditions. Under diffusion control, the etch rate can be increased by either stirring or by increasing the KOH concentration.

Defects can be revealed in a stirred 0.02 M KOH/0.02 M $S_2O_8^{2-}$ solution, for which the short-circuit potential is in the onset range (Fig. 6b). The defects are observed as whiskers and have an average diameter of 45 nm. Several groups have demonstrated that the whiskers are correlated with threading dislocations in the epitaxial GaN

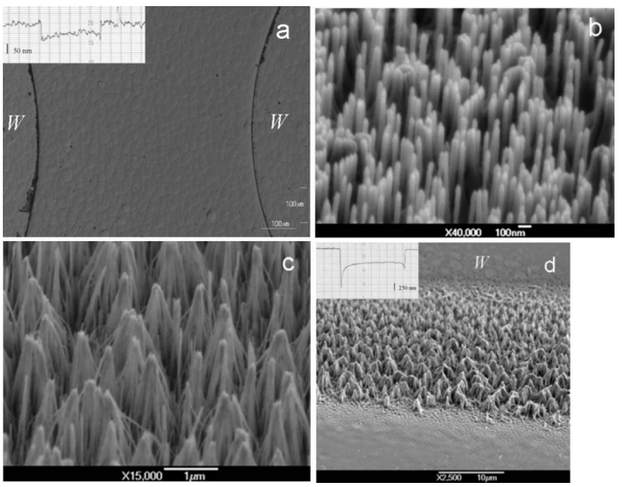

Figure 6. Photogalvanic etching of n-type GaN in alkaline solution. (a) The original smooth surface is maintained after 20 min of etching in an unstirred solution of 0.004 M KOH/0.02 M $S_2O_8^{2-}$; the scale bar corresponds to 100 μm. (b) Etching in a stirred 0.02 M KOH/0.02 M $S_2O_8^{2-}$ solution reveals defects after 5 min. (c) When the concentration of both components is increased to 0.05 M, the etch rate increases and the defects are overetched. (d) With a 0.02 M KOH/0.02 M $S_2O_8^{2-}$ solution (unstirred), defects are revealed at the edges, while the rest of the surface remains polished. [(a) and (d)] The areas denoted as *W* were covered with wax. The insets show surface profiles of the etched area.

layer.[9,33,34] When the concentration ratio is increased to 0.05 M KOH/0.05 M $S_2O_8^{2-}$, the etch rate increases drastically. The defects are significantly overetched, which causes them to bunch (Fig. 6c). Figure 6d shows an image of a GaN sample that was etched for 20 min in an unstirred solution of 0.02 M KOH/0.02 M $S_2O_8^{2-}$. An etch rate of about 25 nm/min is obtained, and the surface finish is smooth in the middle of the groove, even after 500 nm of etching (see the bottom part of Fig. 6d). Larger etch rates are observed at the edges of the groove (inset Fig. 6d) due to an enhanced supply of OH^- ions from the surrounding nonetching area (masked by wax). Furthermore, defects are revealed at the edges, clear from the appearance of (bunched) needles. It is concluded that the etching kinetics vary locally. In the middle of the groove, $\Phi_p > \Phi_{OH}$ and polishing occurs. Enhanced mass transport at the edges results locally in an increased dissolution rate (Φ_{OH} becomes larger than Φ_p). The current plateau of Fig. 5, curve (a), shifts to higher values and a more positive potential, while the slope of the reduction current remains relatively unchanged; U_{SC} is now located in the onset range.

As mentioned above, there have been several reports of an enhancement of photoetch rates of n-type GaN due to direct metallization of the surface. Bardwell and co-workers[15] used a 210 nm sputtered Pt mask on MBE-grown GaN and obtained etch rates approximately 1 order of magnitude higher than those observed using inert masks. By the proper choice of conditions, they were able to control the etched surface morphology. They suggested that a reactive agent ($SO_4^{\bullet-}$ and $OH^\bullet$ radicals) responsible for etching is catalytically generated at the Pt surface. The results presented here suggest an alternative mechanism: The Pt acts as a cathode in a photogalvanic cell, enhancing the photo-oxidation of the GaN anode. For etching to be effective, the contact resistance between Pt and GaN should not be large.[11] While the Pt/GaN contact is not expected to be ohmic, the junction at the GaN/metal edge under photoetching conditions is likely to be leaky. Evidence suggesting that transport of reactive radicals is not the important step in etching is provided by the results of Diaz et al.[18,19] On illuminating n-type GaN provided with 7 nm Pt areas in a $CH_3OH/HF/H_2O$ solution containing H_2O_2, they formed a strongly anisotropic porous structure. (H_2O_2, like $S_2O_8^{2-}$, is a strong two-electron oxidizing agent.) Because the pores were narrow and 2 μm long, radicals formed at the metal on the top surface would have to travel the length of the pore without adsorbing on the walls to ensure pore propagation. This seems unlikely. The photogalvanic mechanism (Fig. 4), originally proposed for Si etching,[35,36] offers a more plausible explanation of these results.

Conclusions

The influence of $S_2O_8^{2-}$ on the photoetching of n-type GaN in KOH solution was investigated by electrochemical methods. The photoanodic dissolution rate decreases upon the addition of $S_2O_8^{2-}$ due to the absorption of high energy photons by the solution. The onset of the cathodic reaction shifts to a positive potential upon the addition of $S_2O_8^{2-}$. As a result, open-circuit photoetching is possible. At negative potentials, $S_2O_8^{2-}$ is reduced and $SO_4^{\bullet-}$ radicals are formed. With EL measurements, we showed that the radicals inject holes into the VB. By using a two-compartment cell, we found that GaN short-circuited to a noble metal acts as a photogalvanic cell. The surface finish after etching is very sensitive to the experimental conditions: concentration, surface area ratio, light intensity, and mass transport.

Acknowledgments

The authors thank Ruud Balkenende of Philips Research for useful discussions and Hans Ligthart and Rinus Mackaay for technical assistance. This work was financially supported by the Dutch Technology Foundation (STW, UPC-6317).

Utrecht University assisted in meeting the publication costs of this article.

References

1. S. Nakamura, S. Pearton, and G. Fasol, *The Blue Laser Diode*, Springer, New York (2000).
2. D. Zhuang and J. H. Edgar, *Mater. Sci. Eng. R.*, **48**, 1 (2005).
3. N. M. Stanton, A. J. Kent, P. Hawker, T. S. Cheng, C. T. Foxon, D. Korakakis, R. P. Campion, C. R. Staddon, and J. R. Middleton, *Mater. Sci. Eng., B*, **68**, 52 (1999).
4. J. Skriniarova, P. Bochem, A. Fox, and P. Kordos, *J. Vac. Sci. Technol. B*, **19**, 1721 (2001).
5. P. H. L. Notten, J. E. A. M. van den Meerakker, and J. J. Kelly, *Etching of III-V Semiconductors*, Elsevier Advanced Technology, Oxford (1991).
6. M. S. Minsky, M. White, and E. L. Hu, *Appl. Phys. Lett.*, **68**, 1531 (1996).
7. C. Youtsey, I. Adesida, and G. Bulman, *Appl. Phys. Lett.*, **71**, 2151 (1997).
8. C. Youtsey, I. Adesida, L. T. Romano, and G. Bulman, *Appl. Phys. Lett.*, **72**, 560 (1998).
9. C. Youtsey, L. T. Romano, and I. Adesida, *Appl. Phys. Lett.*, **73**, 797 (1998).
10. A. R. Stonas, P. Kozodoy, H. Marchand, P. Fini, S. P. DenBaars, U. K. Mishra, and E. L. Hu, *Appl. Phys. Lett.*, **77**, 2610 (2000).
11. L. Macht, J. J. Kelly, J. L. Weyher, A. Grzegorczyk, and P. K. Larsen, *J. Cryst. Growth*, **273**, 347 (2005).
12. A. C. Tamboli, M. C. Schmidt, S. Rajan, J. S. Speck, U. K. Mishra, S. P. DenBaars, and E. L. Hu, *J. Electrochem. Soc.*, **156**, H47 (2009).
13. J. A. Bardwell, I. G. Foulds, J. B. Webb, H. Tang, J. Fraser, S. Moisa, and S. J. Rolfe, *J. Electron. Mater.*, **28**, L24 (1999).
14. H. Maher, D. W. DiSanto, G. Soerensen, C. R. Bolognesi, H. Tang, and J. B. Webb, *Appl. Phys. Lett.*, **77**, 3833 (2000).
15. J. A. Bardwell, J. B. Webb, H. Tang, J. Fraser, and S. Moisa, *J. Appl. Phys.*, **89**, 4142 (2001).
16. Z. H. Hwang, J. M. Hwang, H. L. Hwang, and W. H. Hung, *Appl. Phys. Lett.*, **84**, 3759 (2004).
17. T. L. Rittenhouse, P. W. Bohn, and I. Adesida, *Solid State Commun.*, **126**, 245 (2003).
18. D. J. Diaz, T. L. Williamson, I. Adesida, P. W. Bohn, and R. J. Molnar, *J. Vac. Sci. Technol. B*, **20**, 2375 (2002).
19. D. J. Diaz, T. L. Williamson, I. Adesida, P. W. Bohn, and R. J. Molnar, *J. Appl. Phys.*, **94**, 7526 (2003).
20. R. Memming, *J. Electrochem. Soc.*, **116**, 785 (1969).
21. A. Manivannan and A. Fujishima, *J. Lumin.*, **42**, 43 (1988).
22. A. Manivannan, K. Itoh, K. Hashimoto, T. Sakata, and A. Fujishima, *J. Electrochem. Soc.*, **137**, 3121 (1990).
23. I. M. Huygens, W. P. Gomes, A. Theuwis, and K. Strubbe, *J. Electrochem. Soc.*, **150**, G602 (2003).
24. C. J. Hung, L. I. Halaoui, A. J. Bard, P. A. Grudowski, R. D. Dupuis, J. Molstad, and F. J. DiSalvo, *Electrochem. Solid-State Lett.*, **1**, 142 (1998).
25. I. M. Huygens, K. Strubbe, and W. P. Gomes, *J. Electrochem. Soc.*, **147**, 1797 (2000).
26. J. L. Weyher, D. H. van Dorp, J. J. Kelly, and F. D. Tichelaar, Unpublished.
27. S. S. Kocha, M. W. Peterson, D. J. Arent, J. M. Redwing, M. A. Tischler, and J. A.

Turner, *J. Electrochem. Soc.*, **142**, L238 (1995).
28. T. Rotter, D. Mistele, J. Stemmer, F. Fedler, J. Aderhold, J. Graul, V. Schwegler, C. Kirchner, M. Kamp, and M. Heuken, *Appl. Phys. Lett.*, **76**, 3923 (2000).
29. J. J. Kelly and P. H. L. Notten, *J. Electrochem. Soc.*, **130**, 2452 (1983).
30. L. Macht, J. L. Weyher, A. Grzegorczyk, and P. K. Larsen, *Phys. Rev. B*, **71**, 073309 (2005).
31. C. Hums, T. Finger, T. Hempel, J. Christen, A. Dadgar, A. Hoffmann, and A. Krost, *J. Appl. Phys.*, **101**, 033113 (2007).
32. J. A. Bardwell, I. Foulds, B. Lamontagne, H. Tang, J. B. Webb, P. Marshall, S. J. Rolfe, J. Stapledon, and T. W. MacElwee, *J. Vac. Sci. Technol. A*, **18**, 750 (2000).
33. J. L. Weyher, F. D. Tichelaar, H. W. Zandbergen, L. Macht, and P. R. Hageman, *J. Appl. Phys.*, **90**, 6105 (2001).
34. A. Watanabe, H. Takahashi, T. Tanaka, H. Ota, K. Chikuma, H. Amano, T. Kashima, R. Nakamura, and I. Akasaki, *Jpn. J. Appl. Phys., Part 2*, **38**, L1159 (1999).
35. X. H. Xia, C. M. A. Ashruf, P. J. French, and J. J. Kelly, *Chem. Mater.*, **12**, 1671 (2000).
36. J. J. Kelly, X. H. Xia, C. M. A. Ashruf, and P. J. French, *IEEE Sens. J.*, **1**, 127 (2001).